Journal of Alloys and Compounds 514 (2012) 174–178

Contents lists available at SciVerse ScienceDirect

Journal of Alloys and Compounds

journal homepage: www.elsevier.com/locate/jallcom

Polyol synthesis and characterizations of cubic ZrO_2:Eu^{3+} nanocrystals

S. Dhiren Meetei [a], Sh. Dorendrajit Singh [a,*], V. Sudarsan [b]

[a] Department of Physics, Manipur University, Canchipur-795 003, Imphal, India
[b] Chemistry Division, Bhabha Atomic Research Centre, Mumbai 400 085, India

ARTICLE INFO

Article history:
Received 25 August 2011
Accepted 11 November 2011
Available online 22 November 2011

Keywords:
Polyol synthesis
Characterization
Cubic
Nanocrystal
Charge transfer state

ABSTRACT

Nanocrystalline ZrO_2 and ZrO_2:Eu^{3+} were synthesized by polyol route. The x-ray diffraction (XRD) pattern of ZrO_2 shows presence of both monoclinic and tetragonal phase of zirconia, while that of ZrO_2:Eu^{3+} show cubic structure. Cubic phase is the most desired phase of zirconia. However, it is difficult to distinguish between the tetragonal and cubic phases solely from XRD study. Therefore, the characterizations of cubic phase in the doped samples are substantiated by transmission electron microscopy (TEM), Fourier transform infrared (FT-IR) and photoluminescence (PL) studies. Interplaner spacing, d_{hkl} are calculated from the selected area electron diffraction (SAED) rings and they are found to be consistent with that of cubic zirconia. FT-IR spectra of doped and undoped samples are found to be different. This is attributed to the presence of both monoclinic and tetragonal phase in the undoped sample and only cubic phase in the doped samples. PL excitation and emission spectra of the samples are studied. The asymmetry ratio is found to be less than that of the reported tetragonal phase indicating that the present analyzing samples have higher symmetry than tetragonal phase. Variations of Eu^{3+} emission peaks are observed as that of charge transfer state (CTS).

1. Introduction

Recently nanomaterials and nanocrystals have attracted considerable scientific interest due to their improved properties resulting from grain size refinement in nanometer scale. Different novel properties of materials are revealed at nano regime; their properties can be tuned by their sizes, shapes, etc. [1–5]. In these point of views, nanocrystalline zirconia (ZrO_2) and ZrO_2:Eu^{3+} are synthesized and studied for various applications [6–11]. Zirconia is a technologically important material due to its high melting point, high thermal and mechanical resistance, high thermal expansion coefficient, low thermal conductivity, high thermochemical resistance, high corrosion resistance, high dielectric constant, photothermal stability, etc. [8–11]. High chemical and photochemical stability with high refractive index and low phonon energy makes it an optimized luminescent host [8,10,11]. Therefore, it has extensive applications in photonics and other industries.Zirconia have three crystalline phases, that is, monoclinic (below 1170 °C), tetragonal (1170–2370 °C) and cubic (above 2370 °C) [8,9]. Among these, cubic phase is the most desirable for technical applications [12]. In order to manufacture zirconia components, it is necessary to lock the material wholly or partially into the cubic phase [13]. In fact, the crystal lattice tends to transform into a structure with higher symmetry as the crystallite size decreases [14–19]. As a result, it is an important task to synthesize the crystallite size as small as possible. The synthesis of small crystallite size is achieved by polyol route and it is reported in this work.The assignment of tetragonal and cubic phase solely from the XRD can be misleading [12,14–17]. Because, these two phases have similar XRD patterns. The problem is more pronounced when the peaks are broadening due to small sizes of the crystals [17]. With these views, characterization of cubic phase, especially, nanocrystalline zirconia is a challenging task. Moreover, since the properties of zirconia depend on the crystal structures [6], proper identification of phase is needed for application in various fields and the problems which may arise due to miss identification. Therefore, TEM, FT-IR and PL studies are also reported to substantiate the results from the XRD study. In view of the fact that, electron diffraction is very sensitive to changes in the crystal structure that cannot be detectable through XRD, TEM study is performed to distinguish the tetragonal and cubic zirconia [18]. FT-IR spectroscopy has been widely used in the characterization of different morphologies of ZrO_2 and related materials. It is reported that FT-IR spectra may be more sensitive than XRD in the characterization of the phases of ZrO_2 [20]. Therefore, the samples are further characterized by FT-IR. A considerable amount of works has been done on the PL characterization of monoclinic and tetragonal ZrO2:Eu^{3+} [12,17,21]. However, PL characterization of cumbersome cubic zirconia is limited and need further studies. Here, the PL characterization of cubic zirconia is reported.

* Corresponding author. Tel.: +91 385 2435080; fax: +91 385 2435145.
E-mail address: dorendrajit@yahoo.co.in (Sh.D. Singh).

0925-8388/$ – see front matter © 2011 Elsevier B.V. All rights reserved.
doi:10.1016/j.jallcom.2011.11.051

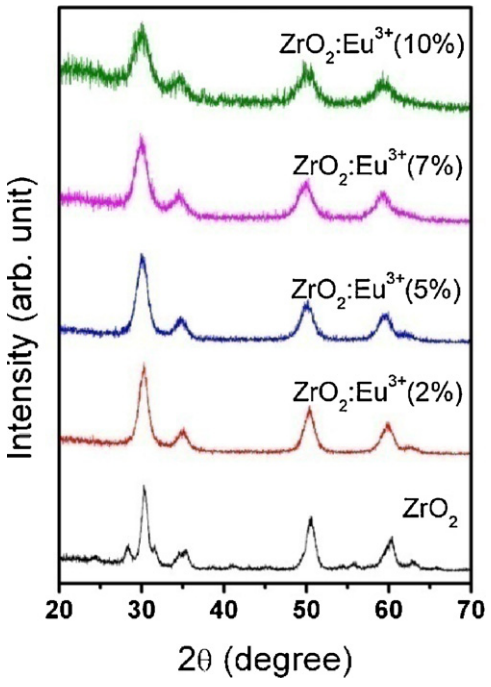

Fig. 1. XRD patterns of undoped ZrO_2 and doped ZrO_2:Eu^{3+} (2, 5, 7 and 10%).

2. Experimental

Undoped ZrO_2 and Eu^{3+} (2, 5, 7 and 10%) doped ZrO_2 nanocrystals were synthesized effectively by polyol method. Ethylene glycol (EG) and polyethylene glycol (PEG) were used as reaction medium and capping agent. For synthesis of ZrO_2:Eu^{3+} (2%), 2 g of $ZrOSO_4$ was introduced in 10 ml of deionized water by warming at 50 °C to dissolve it. Then, 70.68 mg of Eu_2O_3 was introduced to dissolve in the solution. After that, the solution is treated with another solution of PEG (10 g), EG (50 ml) and urea (10 g) warm at 50 °C. The whole solution is then heated at 120 °C, temperature at which precipitate formation took place, for 30 min. The precipitate was collected as gel by centrifugation. The gel so obtained is annealed at 500 °C for 4 h in ambient atmosphere. Similar procedures were performed for synthesis of other samples.

The X-ray diffraction (XRD) data are recorded in PANalytical diffractometer at 40 kV and 30 mA. The wavelength used is that of Cu K_α (1.54060 Å). Transmission electron microscopy (TEM) images were recorded using JEM-2000FX microscope (JEOL) at 160.0 kV. Fourier transform infra-red (FT-IR) spectra were recorded in MB 102 spectrometer (BOMEN). Photoluminescence (PL) emission and excitation spectra were obtained from LS55 fluorometer (Perkin Elmer). All the measurements were recorded at room temperature.

3. Results and discussion

Fig. 1 shows the XRD patterns of undoped ZrO_2 and doped ZrO_2:Eu^{3+} (2, 5, 7 and 10%) samples. Due to nanocrystalline nature of the samples, the patterns show a significant peak broadening. From X'pert HighScore's search match analysis, undoped ZrO_2, shows the presence of both tetragonal *P4₂/nmc (137)* (Ref. Code: 01-079-1770) and *P2₁/c* (14) monoclinic (Ref. Code: 01-083-0944) phases. The percentage of monoclinic to tetragonal phase quantified from the X'pert HighScore is 43/57. However, the patterns of Eu^{3+} doped samples show *Fm3m* (2 2 5) cubic phase (Ref. Code: 00-049-1642). It is reported that most of the XRD peaks of the tetragonal and cubic phase of zirconia are overlapped and it is very difficult to distinguish between the two from XRD patterns [12,14–17]. Meanwhile, reports have been found that the crystal lattice tends to transform into a structure with higher symmetry, cubic phase, as the crystallite size decreases [15,19]. Therefore, to observe the crystallite sizes, Scherrer equation: $t = (0.9\lambda)/(\beta \cos\theta)$ is employed; where 0.9 is shape factor, λ is the X-ray wavelength, β is line broadening at half the maximum intensity in radians, and θ is the Bragg angle. As expected, the crystallite sizes are found to decrease with increase in Eu^{3+} concentration (Table 1). This can also be visualized from the intensities of XRD patterns shown in Fig. 2. That is, the intensity decreases indicating that the crystallite size decreases. Therefore, our proposition that the crystal structures of doped samples are cubic but not tetragonal is likely. This will further be substantiated from TEM, FT-IR and PL studies.

Table 1
Crystallite sizes and unit cell parameters of the samples.

Sl. No.	Sample	Size (nm)	Unit cell parameters	
			a (Å)	Cell volume (Å^3)
1	ZrO_2	12	–	–
2	ZrO_2:Eu^{3+} (2%)	7	5.13	134.91
3	ZrO_2:Eu^{3+} (5%)	6	5.16	137.04
4	ZrO_2:Eu^{3+} (7%)	5	5.17	138.31
5	ZrO_2:Eu^{3+} (10%)	4	5.19	139.46

Unit cell parameters of the samples are calculated from the XRD data. Unit cell volume and lattice parameter are found to increase with increase in Eu^{3+}. Moreover, with increase in doping concentration, the shift in diffraction peaks positions (Fig. 2) towards the lower diffraction angle is observed. These are attributed to the substitution of smaller Zr^{4+} (ionic radius = 87 pm) by Eu^{3+} (ionic radius = 98 pm) [14]. This established our intention to dope Eu^{3+} in ZrO_2.

The TEM image of ZrO_2:Eu^{3+} (2%) and its corresponding SAED image are shown in Fig. 3(a) and (b) respectively. It is observed from the TEM image that particles are distributed uniformly. Crystallinity of the sample is confirmed from the SAED image. From the diffraction rings of SAED image, interplaner spacing, d_{hkl} are calculated by using camera equation: $d_{hkl} = (L\lambda')/R$, where L = camera length, 100 cm; λ' = wavelength of electron, 0.0306 Å and R = radius of diffraction rings. The calculated d_{hkl} values of the four main diffraction rings are 2.96, 2.56, 1.81 and 1.54 Å. These d_{hkl} values agree well, respectively, with that of (1 1 1), (2 0 0), (2 2 0) and (3 1 1) corresponding to ICDD PDF Ref. Code: 00-049-1642, which is cubic.

The FT-IR spectra of the samples are shown in Fig. 4(a). All samples exhibit bands at 3420 and 1655 cm^{-1} assigned to the bending vibration and stretching vibration of the O–H bond in absorbed and coordinated water, showing that there is residual structural OH. Below 1000 cm^{-1}, there is a sharp fall in transmittance spectra. To observe characteristic vibration bands due to ZrO_2 and to identify either the phase is tetragonal or cubic or both; FT-IR spectra of ZrO_2 and ZrO_2:Eu^{3+}(2%) samples are shown within 300–900 cm^{-1} in Fig. 4(b). The spectrum of ZrO_2, where both monoclinic and tetragonal phases co-exist, shows bands at 354, 455, 498, 575, and 741 cm^{-1}. The bands at 354, 498 and 741 cm^{-1} correspond to the monoclinic phase and that at 455 and 575 cm^{-1} are

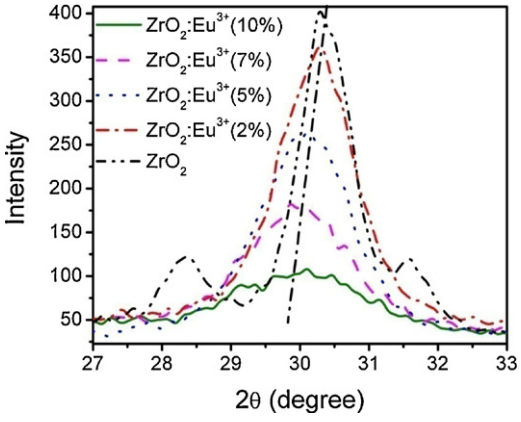

Fig. 2. XRD patterns of the samples showing shift in peak intensity and peak position with increase in Eu^{3+} concentration.

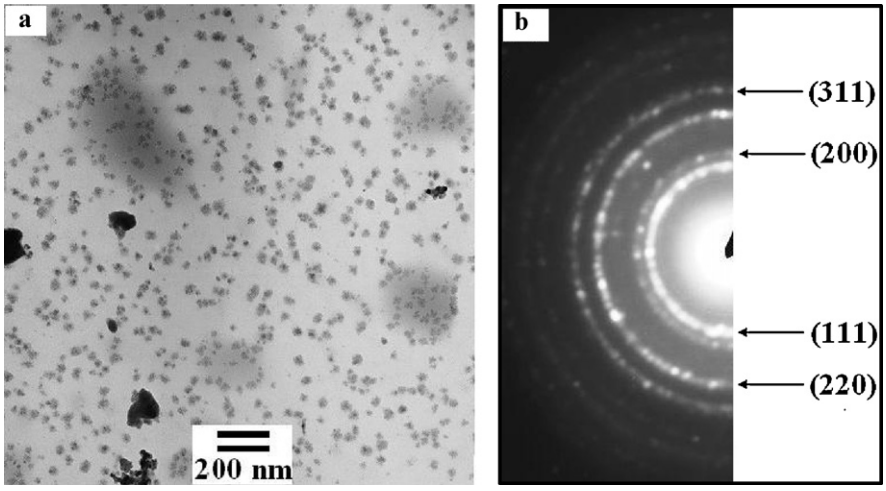

Fig. 3. (a) TEM image of ZrO_2:Eu^{3+} (2%) and its (b) SAED image showing (*h k l*) values.

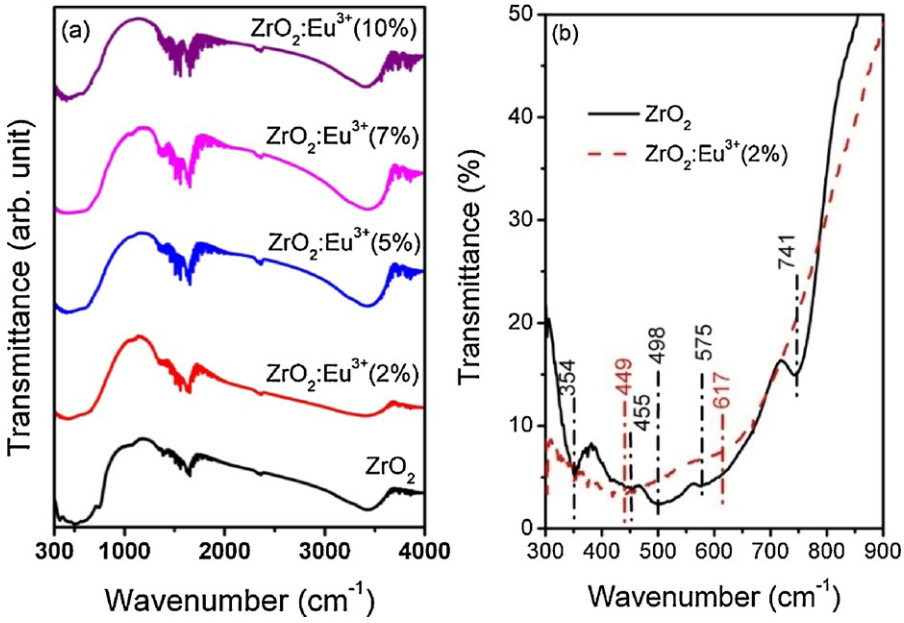

Fig. 4. (a) FT-IR spectra of ZrO_2 and ZrO_2:Eu^{3+} samples. (b) Enlarged view of FT-IR spectra for ZrO_2 and ZrO_2:Eu^{3+} (2%) samples.

related to tetragonal phase of zirconia [20–25]. However, the sample ZrO_2:Eu^{3+}(2%), where existence of cubic phase or tetragonal phase is uncertain, shows no bands due to tetragonal phase. Rather a broad band at 449 cm^{-1} and a shoulder at 617 cm^{-1} are observed. This is consistent with the conclusion that for cubic zirconia only one fundamental mode is active in IR [23]. The same phenomena happened in other doped samples. This confirmed our proposition that the doped samples are cubic but not tetragonal.

Fig. 5 shows the excitation spectra of ZrO_2:Eu^{3+} (2, 5, 7 and10%), recorded under 613 nm emission wavelength. The peak within 231–307 nm is due to charge transfer state (CTS) of Eu^{3+}, which originates from interaction between Eu^{3+} and O^{2-} [12]. It is clearly observed from the figure that peak position and intensity changes with change in Eu^{3+} concentration. The peak position and intensity of ZrO_2:Eu^{3+} (2%) and ZrO_2:Eu^{3+} (5%) are almost same. However, the peak position of ZrO_2:Eu^{3+} (7%) and ZrO_2:Eu^{3+} (10%) shift towards lower and higher wavelength, respectively. While the peak intensity increases with increase in Eu^{3+} concentration. These variations in CTS peak position and intensity are summarized in Table 2. It is reported that Eu–O bond distance is a factor that strongly determine the CTS position in the case of cubic phase [26]. Therefore, the variation in peak position and intensity can be attributed to variation in bond length of Eu–O [12,26]. With increase in bond length the peak shifts towards higher wavelength while the peak intensity decreases [12,26].

Table 2
Peak intensities and positions of CTS, electric and magnetic dipole transitions of Eu^{3+} in the cubic ZrO_2:Eu^{3+} samples. The number 1.05/267 represent: peak intensity ≡ 1.05 and peak position ≡ 267 and so forth.

Sl. No.	Sample	Intensity			
		CTS	$^5D_0 \rightarrow {}^7F_2$ (*E*)	$^5D_0 \rightarrow {}^7F_1$ (*M*)	*E*/*M*
1	ZrO_2:Eu^{3+}(2%)	1.05/267	1.20/612	0.95/592	1.26
2	ZrO_2:Eu^{3+}(5%)	1.05/269	1.17/609	0.93/591	1.25
3	ZrO_2:Eu^{3+}(7%)	1.17/258	1.44/607	1.24/590	1.16
4	ZrO_2:Eu^{3+}(10%)	1.60/272	1.73/615	1.41/593	1.23

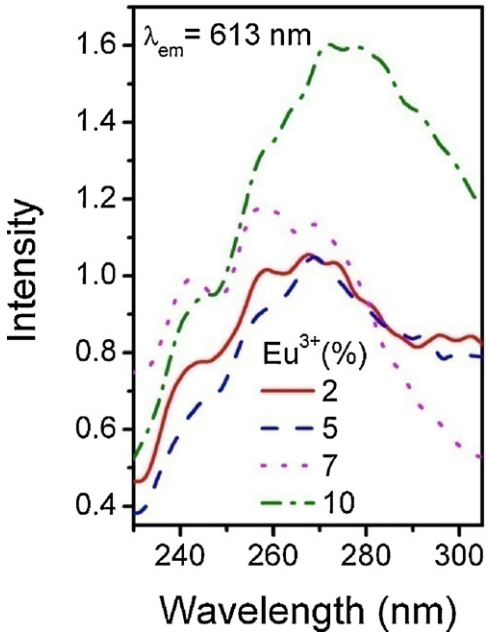

Fig. 5. Charge transfer state (CTS) of Eu^{3+} in ZrO_2:Eu^{3+} samples recorded under 613 nm emission wavelength.

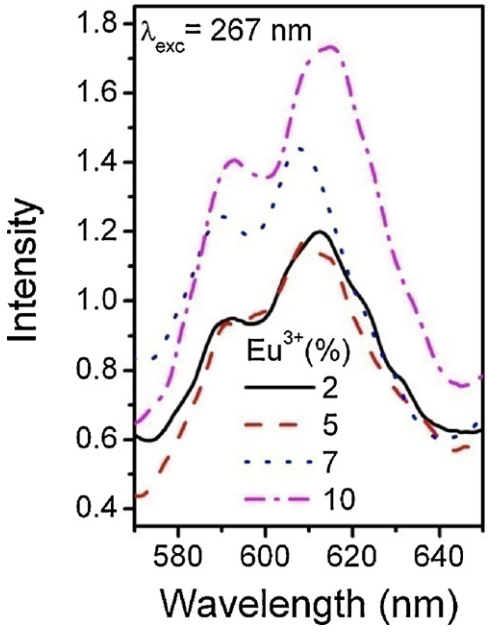

Fig. 6. PL emission spectra of Eu^{3+} in ZrO_2:Eu^{3+} samples recorded under 267 nm excitation wavelength.

The PL emission spectra of ZrO_2:Eu^{3+} samples recorded under 267 nm excitation wavelength are shown in Fig. 6. It is observed from this figure that the samples show two peaks due to Eu^{3+} between 580 and 640 nm. The first peak originated from magnetic dipole transition (M), $^5D_0 \rightarrow {}^7F_1$, while the other is originated from structurally sensitive electric dipole transition (E), $^5D_0 \rightarrow {}^7F_2$ of Eu^{3+}. The position of the first peak varies from 590 to 593 nm while that of the second peak varies from 607 to 615 nm. The variation of the peak position is more prominent for the later peak. It is to be noted that $^5D_0 \rightarrow {}^7F_2$ transition is highly sensitive to structural change and environment effects and the difference of $^5D_0 \rightarrow {}^7F_2$ emission peaks in relative positions was due to the difference of the effects of the crystal field perturbation on the individual f-f transitions [12]. On the other hand, the emission peaks intensities are almost same for ZrO_2:Eu^{3+} (2%) and ZrO_2:Eu^{3+} (5%). However, higher Eu^{3+} doped samples show increase in peak intensity. The variations in the emission peak intensity and position is similar to that of CTS, discussed above. That is, the shift in CTS peak position towards higher wavelength results in the shift of emission peaks towards the higher wavelength. And increase in peak intensity of CTS is consistent with the increase in emission peak intensity. These correlations can be clearly observed from Figs. 5, 6 and Table 2. Consequently, it is expected that the variation of Eu^{3+} emission peak positions and intensity might also related with the Eu–O bond length as in the case of CTS peak. But no reports are found for the same.

The asymmetry ratio of structurally sensitive electric dipole transition, $^5D_0 \rightarrow {}^7F_2$ and magnetic dipole transition, $^5D_0 \rightarrow {}^7F_1$ (E/M) strongly depends on the local symmetry of the Eu^{3+} [12,15]. And a higher symmetry of the crystal field around Eu^{3+} will results in a lower E/M value [12]. To understand the symmetry of the sample, E/M is calculated (Table 1). The highest value of E/M obtained is 1.26. This value is less than that of reported tetragonal phase. The reported E/M value is 1.46 for tetragonal [15]. Therefore, the symmetry of Eu^{3+} site in the present analyzing sample is higher than tetragonal phase. The phase which has higher symmetry than tetragonal is cubic phase. Therefore, the notion of E/M supports the doped samples to be cubic in phase.

4. Conclusions

By polyol method, ZrO_2 and cubic ZrO_2:Eu^{3+} nanocrystalline were synthesized at significantly lower temperature than reported temperature. The sizes of the particles are within the range 4–12 nm. Both monoclinic and tetragonal phases are present in undoped ZrO_2. Only cubic phase is present in doped ZrO_2:Eu^{3+}. The characterizations of cubic phase were done effectively by XRD, TEM, FT-IR and PL studies. They are consistent with each other. From the PL studies, Eu^{3+} emission peak position and intensity variations were found to be consistent with that of the CTS. Hence, it is expected in cubic zirconia that the variation of Eu^{3+} emission peak positions and intensity might also related with the Eu–O bond length. This nano-sized cubic phase ZrO_2:Eu^{3+} may have important application in fabricating devices.

Acknowledgements

The authors thank R.S. Ningthoujam and N. Shanta Singh for useful discussion. This research project is supported financially by the Department of Atomic Energy (DAE), Government of India (Sanction Number 2008/37/35/BRNS).

References

[1] T. Jovanovic-Talisman, A. Zilman, Nat. Nanotechnol. 6 (2011) 397.
[2] N. Fournier, C. Wagner, C. Weiss, R. Temirov, F.S. Tautz, Phys. Rev. B 84 (2011) 035435.
[3] G. Sallen, A. Tribu, T. Aichele, R. André, L. Besombes, C. Bougerol, M. Richard, S. Tatarenko, K. Kheng, J.P. Poizat, Phys. Rev. B 84 (2011) 041405.
[4] C. Tang, G. Alici, J. Phys. D: Appl. Phys. 44 (2011) 335502.
[5] A. Smolyanitsky, V.K Tewary, J. Phys.: Condens. Matter. 23 (2011) 355006.
[6] L. Kumari, W. Li, D. Wang, Nanotechnology 19 (2008) 195602.
[7] H. Cao, X. Qiu, B. Luo, Y. Liang, Y. Zhang, R. Tan, M. Zhao, Adv. Funct. Mater. 14 (2004) 243.
[8] R. Gillani, B. Ercan, A. Qiao, T.J. Webster, Int. J. Nanomed. 5 (2010) 1.
[9] Y. Al-Khatatbeh, K.K.M. Lee, B. Kiefer, Phys. Rev. B 81 (2010) 214102.
[10] E. De la Rosa, L.A. Diaz-Torres, P. Salas, R.A. Rodríguez, Opt. Mater. 27 (2005) 1320.
[11] H.D.E. Harrison, N.T. McLamed, E.C. Subbarao, J. Electrochem. Soc. 110 (1963) 23.
[12] L. Chen, Y. Liu, Y. Li, J. Alloys Compd. 381 (2004) 266.
[13] http://www.azom.com/Details.asp?ArticleID=133.

[14] K. Kuratani, M. Mizuhata, A. Kajinami, S. Deki, J. Alloys Compd. 408/412 (2006) 711.
[15] B.K. Moon, I.M. Kwon, J.H. Jeong, C.K. Kim, S.S. Yi, P.S. Kim, H. Choi, J.H. Kim, J. Lumin. 122/123 (2007) 855.
[16] A. Benyagoub, Phys. Rev. B 72 (2005) 094114.
[17] J. Joo, T. Yu, Y.W. Kim, H.M. Park, F. Wu, J.Z. Zhang, T. Hyeon, J. Am. Chem. Soc. 125 (2003) 6553.
[18] http://www.eng.uc.edu/~gbeaucag/Classes/XRD/Labs/Keithhtml/Keith.html.
[19] P. Ayyub, V.R. Palkar, S. Chattopadhyay, M. Multani, Phys. Rev. B 51 (1995) 6135.
[20] H. Zhang, Y. Liu, K. Zhu, G. Siu, Y. Xiong, C. Xiong, J. Phys.: Condens. Matter. 11 (1999) 2035.
[21] Z.W. Quan, L.S. Wang, J. Lin, Mater. Res. Bull. 40 (2005) 810.
[22] http://www.azom.com/Details.asp?ArticleID=4307#14.
[23] S.F. Wang, F. Gu, M.K. Lü, Z.S. Yang, G.J. Zhou, H.P. Zhang, Y.Y. Zhou, S.M. Wang, Opt. Mater. 28 (2006) 1222.
[24] F. Heshmatpour, R.B. Aghakhanpour, Powder Technol. 205 (2011) 193.
[25] H.R. Pouretedal, M. Hosseini, Acta Chim. Slov. 57 (2010) 415.
[26] H.E. Hoefdraad, J. Solid State Chem. 15 (1975) 175.